



Nolan, Steven P and Nelson, David James and Gómez-Suárez, Adrián (2017) Quantifying and understanding the steric properties of N-heterocyclic carbenes. Chemical Communications. ISSN 1359-7345 ,

This version is available at <https://strathprints.strath.ac.uk/59766/>

Strathprints is designed to allow users to access the research output of the University of Strathclyde. Unless otherwise explicitly stated on the manuscript, Copyright © and Moral Rights for the papers on this site are retained by the individual authors and/or other copyright owners. Please check the manuscript for details of any other licences that may have been applied. You may not engage in further distribution of the material for any profitmaking activities or any commercial gain. You may freely distribute both the url (<https://strathprints.strath.ac.uk/>) and the content of this paper for research or private study, educational, or not-for-profit purposes without prior permission or charge.

Any correspondence concerning this service should be sent to the Strathprints administrator: strathprints@strath.ac.uk

The Strathprints institutional repository (<https://strathprints.strath.ac.uk>) is a digital archive of University of Strathclyde research outputs. It has been developed to disseminate open access research outputs, expose data about those outputs, and enable the management and persistent access to Strathclyde's intellectual output.

Quantifying and understanding the steric properties of *N*-heterocyclic carbenes

 Adrián Gómez-Suárez,^a David J. Nelson,^b and Steven P. Nolan^c

 Received 00th January 20xx,
Accepted 00th January 20xx

DOI: 10.1039/x0xx00000x

www.rsc.org/

This Feature Article presents and discusses the use of different methods to quantify and explore the steric impact of *N*-heterocyclic carbene (NHC) ligands. These include a) the *percent buried volume* (% V_{bur}), which provides a convenient single number to measure steric impact and b) *steric maps*, which provide a graphical representation of the steric profile of a ligand using colour-coded contour maps. A critical discussion of the scope and limitations of these tools is presented, along with some examples of their use in organometallic chemistry and catalysis. This Article should provide all users of NHCs, from organic, organometallic, and inorganic chemistry backgrounds, with an appreciation of how these tools can be used to quantify and compare their steric properties.

1. Introduction

The use of *N*-heterocyclic carbenes (NHC) within the chemical sciences is now widespread;¹ these exciting species find applications in transition metal chemistry (the primary focus of this review),² as organocatalysts,³ and as reagents to stabilise intriguing geometries and oxidation states of main group elements.² The ease of synthesis of the most common classes of NHCs and the flexibility of these synthetic routes have allowed researchers to prepare and characterise a very large number of examples. The challenge is often to select the right NHC for each application; one way in which this can be approached is to consider important properties of the carbene⁴ and make a rational and informed decision based on how these properties affect structure and reactivity. Two of the most important characteristics are *electronic properties* – the ways in which these can be measured have been reviewed recently⁵ – and the *steric properties*.⁶ The measurement of the latter can be complicated by a number of factors. We seek methods to quantify the steric properties of NHCs that are reproducible, physically meaningful, and easy to understand and use. While many phosphines can often be characterised by their cone angle,⁷ NHCs tend to be rather less symmetrical and their steric impact can be unevenly distributed. In addition, the structural flexibility of many NHCs, and their ability to adapt their conformation depending on the other ligands attached to the metal centre, can make it difficult to describe steric properties with a single number.

To overcome the lack of useful and quantitative descriptors to evaluate and compare the steric impact of NHC ligands, the concepts of *percent buried volume* (% V_{bur}) and *steric maps* have been developed (Figure 1).⁸ While both parameters have proven to be useful they have their limitations, as they require either a CIF or XYZ file with the atomic co-ordinates of the desired NHC-bearing species. Metal-ligand bond lengths vary, and X-ray and DFT techniques only provide one (typically static) structure for a complex, which may be strongly influenced by factors such as intermolecular interactions in the crystal lattice or the level of theory that is selected for molecular modelling.

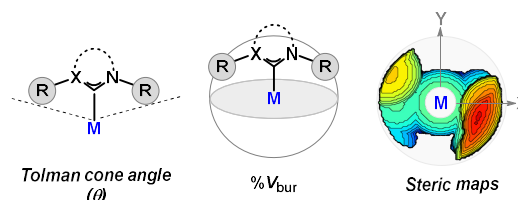


Figure 1. Ways of evaluating the steric impact of NHC ligands.

It is therefore important that chemists who are working with NHCs appreciate the methodologies to describe their steric properties and, importantly, what the limitations of these methods are. This manuscript will, in turn, a) describe and appraise both percent buried volume (% V_{bur}) and steric maps, and b) discuss how these descriptors can be used to provide greater insight into the reactivity of NHCs and compounds that bear them. Other more complex methods of characterising NHCs exist, such as PCA methods that involve a larger number of descriptors,⁹ but the percent buried volume and steric maps are much more accessible and widely used tools as they do not require the use of statistical methods.

^a Organic Chemistry Institute, WWU Münster, Corrensstrasse 40, 48149 Münster, Germany.

^b WestCHEM Department of Pure and Applied Chemistry, University of Strathclyde, Thomas Graham Building, 295 Cathedral Street, Glasgow, G1 1XL, UK.

^c Department of Inorganic and Physical Chemistry, Ghent University, Krijgslaan 281 – S3, 9000 Gent, Belgium.

2. Percent Buried Volume (% V_{bur})

2.1 Definition and Calculation

The percent buried volume (% V_{bur}) is defined as the percentage of a sphere ($r = 3.5 \text{ \AA}$) around the metal centre that is occupied by a given ligand (Figure 2). This is most often determined using a metal-ligand bond length of 2.00 or 2.28 \AA . Hydrogen atoms are typically omitted from the calculation because of their small size and the fact that they are often incorporated in crystal structures using the riding model. The atomic radii of different atoms are determined using scaled Bondi radii, as recommended by Cavallo.^{8b} The use of these default settings is advised, as this allows for better comparisons to be made with the wider literature.

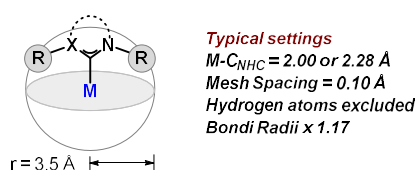


Figure 2. A graphical representation of the definition of the Percent Buried Volume (% V_{bur}).

The use of % V_{bur} to determine steric bulk has several advantages. It does not require the ligand to adopt a symmetrical appropriate geometrical shape (such as a cone, for the Tolman Cone Angle).⁷ It can describe mono- and polydentate ligands, as well as phosphines where the phosphorus bears more than one type of group, such as the widely used Buchwald-type phosphine ligands.¹⁰

The most straightforward method to calculate % V_{bur} is to use the SambVca tool, which is freely available on the Internet.^{8d} Initial versions only provided a buried volume,^{8b} but newer versions of this tool generate steric maps and *per-quadrant* measurements of buried volume, which is useful because NHCs are not always symmetrical (*vide infra*).^{8d} The required input is a CIF or XYZ file with the atomic co-ordinates of either the ligand of interest or the complete complex. While % V_{bur} provides a convenient single number that can be used to quantify the steric impact of each ligand, it is also possible to split this into quadrants. This allows any significant asymmetry in the distribution of steric bulk to be identified.

2.2 Scope and Limitations

It is important to consider the scope and limitations of the percent buried volume so that it can be used appropriately. The main limitation of the % V_{bur} is that while it can be applied to essentially any ligand, regardless of its shape or denticity,⁶ it represents only that conformation. Therefore, the % V_{bur} is highly dependent on good X-ray or DFT data. If a high energy conformer is located by DFT and a lower energy conformer exists, the % V_{bur} data may be misleading. Similarly, poor quality X-ray data with large thermal ellipsoids may not provide a good estimate of the buried volume. In addition, the coordination environment of the metal centre significantly affects the % V_{bur}

of most ligands unless they are particularly rigid: for example, IBioxMe₄ and IBiox6 ligands are often employed due to their structural rigidity (Figure 3). Linear two-coordinate complexes such as [AuCl(NHC)] are often used to measure % V_{bur} for new ligands because these allow the ligand to adopt its preferred conformation without steric clashes between it and other ligands on the metal centre.¹¹ For complexes with higher coordination numbers (i.e. essentially those other than some zerovalent group 10 metals or coinage metals in the +1 oxidation state), steric clashes or dispersive interactions with other ligands will limit the available conformational space. In order to get meaningful information, it is only possible to compare % V_{bur} between complexes of the same metal, coordination number, and geometry.

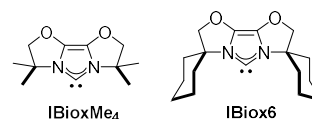


Figure 3. Rigid IBioxMe₄ and IBiox6 ligands.

When comparing the steric hindrance offered by NHC ligands on complexes with similar % V_{bur} it is sometimes difficult to appreciate what constitutes a meaningful difference. To critically assess the limits of the precision of % V_{bur} , data was collected from the CCDC for two NHC ligands – IMes and IPr – in complexes of main group elements and transition metals. These ligands were selected due to their ubiquity in main group chemistry and in transition metal mediated catalysis. These data were filtered to yield only very high quality datasets ($R < 0.05$) and those with more than one independent molecule in the unit cell ($Z' \geq 2$). Comparing % V_{bur} for each NHC ligand in each independent molecule for each CCDC entry provides an estimate of the error in determining % V_{bur} . Only the crystal packing arrangement should vary between structures. Data gathered for these complexes can be found in the Supporting Information. The error in % V_{bur} determination was estimated by considering the range of values for % V_{bur} for each structure in the file; this varied from 0.1 to 2.4%, with slightly smaller ranges for values obtained at a metal-carbon bond length of 2.28 \AA . The mean error was 0.6% at 2.00 \AA and 0.5% at 2.28 \AA , while the median values were 0.4% and 0.3%, respectively. For IPr-containing complexes the errors were much larger, possibly due to the increased flexibility afforded by the *isopropyl* groups. The mean error was 1.4% and the median was 1.2%, at both 2.00 and 2.28 \AA . Based on these data, we would advise caution if drawing conclusions based on buried volumes with differences of less than *ca.* 0.5% for relatively rigid ligands or *ca.* 1.2% for more flexible systems (Figure 4).

[M(NHC)]	Error calculated for % V_{bur} for M-NHC bond length at		Typical settings $M-C_{NHC} = 2.00 \text{ or } 2.28 \text{ \AA}$ Mesh Spacing = 0.10 \AA Hydrogen atoms excluded Bondi Radii x 1.17 Quality of data ($R < 0.05$) Num. molecules per unit cell ($Z' > 2$)
	2.00 \AA	2.28 \AA	
IMes	0.6%	0.5%	
IPr	1.4%	1.4%	

Figure 4. Limits of precision of % V_{bur}

Once the error on the % V_{bur} was estimated, we decided to explore how different substitution patterns affect the steric bulk of a given ligand core. We focussed our attention on alterations made to the backbone, ring size and *N*-alkyl as well as *N*-aryl substituents of NHC ligands. As mentioned above, [AuCl(NHC)] have become a popular way to characterise the % V_{bur} of new NHC ligands due to their linear geometry; thus, we decided to use this type of metal complex to evaluate how the modification of NHC ligands affects the % V_{bur} . In addition, the buried volume is more accurate to describe symmetric ligands, as it represents their overall steric impact. In order to be able to evaluate the influence of systematic modifications on a ligand core, we decided to only collect data for symmetrical NHCs (for a discussion of unsymmetrical NHC ligands, see section 3.2). Data were gathered from the CCDC database and % V_{bur} were calculated for NHC-metal bond lengths of 2.00 and 2.28 Å.

2.2.1 Imidazol-2-ylidenes and Ring-Expanded Analogues

N-substituted imidazol-2-ylidenes represent the most common class of NHCs for organometallic chemistry and metal-mediated catalysis.^{1-2, 4} The related 'ring-expanded' species are also finding interesting applications in organometallic synthesis and catalysis.¹² Two key ways in which the steric profile of these species can be altered are presented and discussed.

Backbone & Ring Size Modifications. In order to assess how tuning the backbone of an NHC ligand would affect its overall steric impact on the metal centre, modifications made to the IPr, IDM and *l*Pr architectures were evaluated using SambVca (Table 1).^{8d} Tuning the backbone of the IPr core with Me or Cl substituents has a negligible influence on the % V_{bur} of the complexes (Entries 1-3, Table 1).¹³ The same trend was observed when examining species bearing IDM derivatives (Entries 7-11, Table 1).¹⁴ However, when examining a more flexible ligand core, such as *l*Pr, installing Me substituents on the backbone results in a considerable change to % V_{bur} (25.5 vs 38.5), while other modifications seem to have little influence (Entries 12-15, Table 1).^{14b, 15} Backbone substituents are often installed with the aim of tuning the electronic properties of NHCs; IPr^{Cl} has a TEP of 2055 cm⁻¹ while IPr is more electron donating at 2050 cm⁻¹, for example. The % V_{bur} calculations show that this type of backbone modification can alter the electronic properties of the ligand without significant perturbation of the steric properties, which might be of interest when designing a new and more efficient catalyst for a particular application. Interestingly, one factor that has a clear impact on the steric influence of IPr derivatives is the saturation of the backbone; for example, the % V_{bur} of SiPr is 1.6% higher than that of IPr. This might be due to the more flexible nature of the 4,5-dihydroimidazol-2-ylidene core compared to the imidazol-2-ylidene. This same reasoning would explain why the steric hindrance increases with the ring size of the NHC ligand, as can be observed when measuring the % V_{bur} of SiPr, THP-Dipp and THD-Dipp (47.0, 50.9 and 52.7, respectively) (Entries 4-6, Table 1).^{14b, 16} In addition, the larger ring size will push the *N*-substituents downwards, towards the metal centre.

Entry	[AuCl(NHC)]	Abbreviation	Reference/ CCDC	% V_{bur} for M-NHC length at	
				2.00 Å	2.28 Å
1		IPr (R = H)	13a 258274	45.4	39.0
2		IPr ^{Me} (R = Me)	13b 727082	44.4	38.9
3		IPr ^{Cl} (R = Cl)	13c 743941	44.9	39.4
4		SiPr	14b 263605	47.0	41.5
5		THP-Dipp	16a 715730	50.9	45.5
6		THD-Dipp	16b 925342	52.7	47.4
7		IDM (R = H)	14a 264465	26.3	22.6
8		IDM ^{Me} (R = Me)	14b 263607	26.2	22.6
9		IDM ^{Cl} (R = Cl)	14c 922326	26.3	22.7
10			14d 728048	26.6	23.0
11			14e 826912	26.5	22.9
12		<i>l</i> Pr (R = H)	15a 250395	27.5	23.5
13		<i>l</i> Pr ^{Me} (R = Me)	15b 263606	38.5	33.9
14		SiPr	15b 1430188	28.2	24.2
15		SiPr ^{Benz}	15c 664618	28.5	24.4

Table 1. Systematic modifications on the backbone of selected NHC ligands and their steric impact on the corresponding [AuCl(NHC)] species.

In summary, when an increase on the steric demand of a given NHC architecture is sought, modifications at the backbone have relatively small effects in the case of rigid (unsaturated) ligands. However, if the flexibility of the system is increased, dramatic changes in the buried volume can be achieved with small modifications.

***N*-substituent Modifications.** When considering the *N*-substitution patterns of NHCs, two distinctive subgroups can be identified: those bearing *N*-aryl substituents and those with *N*-alkyl substituents. The former are generally bulkier and more rigid than the latter, and represent the main class of NHC ligands in organometallic chemistry. However, *N*-alkyl NHCs such as ICy have recently been shown to be promising ligands for the nickel-catalysed cross-coupling of aryl ethers,¹⁷ despite the potentially reduced stability of nickel complexes bearing ICy.¹⁸

Due to the inherent rigidity of the most common and synthetically-accessible imidazol-2-ylidene core, there are a limited number of strategies that can be followed to modify the

steric demand of NHCs bearing *N*-aryl substituents. The main approach to modify the buried volume of these species is to vary the nature of the *ortho*-substituent of the aryl ring. The % V_{bur} dramatically increases when the size of the *ortho*-substituent is increased; on moving from IMes (with 2,4,6-trimethylphenyl *N*-substituents) to IPr (with 2,6-diisopropylphenyl *N*-substituents) the buried volume increases from 36.5% to 45.4% (Entries 1, Tables 1 and 2).^{14b} Further increases in the size of substituents continues this trend: the ITent (IPent, IHept and INon) ligand series represent larger analogues of IPr (Entries 2-4, Table 2).^{11b, 11d} The study of these ligands showed that the larger *ortho*-substituents increase the percent buried volume up to a point. Once the alkyl chain becomes sufficiently long, such as in INon, it no longer affects the overall steric impact of the ligand because the substituents are sufficiently flexible to avoid the metal centre. By convention, the percent buried volume considers a sphere with a radius of 3.5 Å because this is the first coordination sphere of the metal and therefore the area in which most steps of catalysis are likely to take place. Another modification consists of installing larger and/or more rigid groups at the *ortho*-position, such as in IPr* (Entry 5, Table 2).¹⁹ This dramatically increases % V_{bur} , but results in a more rigid ligand than the ITent series. Tuning of the *N*-aryl substituents at the *meta*- and *para*-positions is possible but these modifications generally have little impact on the buried volume as they are far away from the metal centre (Entries 6-7, Table 2).^{11c, 20} In summary, the % V_{bur} for *N*-aryl substituents increases as follows: IMes < IPr ≈ IPr^{OMe} ≈ IPr^{NH2} < IPent < IPr* < IHept ≈ INon; where bulky and flexible substituents on the *ortho*-position of the aryl group have the largest effect on the % V_{bur} .

For *N*-alkyl substituents the effect on the buried volume can be directly linked to the number of substituents on the *ipso* carbon as well as its flexibility. % V_{bur} increases in the order IDM < IPr < ICy < IDD < IAd ≈ I^tBu (Entries 7, 12, Table 1; and Entries 8-11, Table 2).^{14a, 14b, 15b, 21} It is worth noting that large cycloalkyl substituents, such as cyclododecyl groups, have been shown to be very flexible and can adapt their steric bulk depending on the structure of the complex. This effect has been described for iridium and platinum species bearing such ligands.²²

2.2.2 Other Classes of NHC Ligand

It is useful to provide buried volumes for a series of [AuCl(NHC)] species bearing less common NHC ligands, in order to increase the available data on these complexes and allow a comparison with imidazol-2-ylidenes. Table 3 shows a summary of % V_{bur} for a series of gold(I) complexes bearing imidazo[1,5-*a*]pyridinylidene (Entries 1-4, Table 3),²³ bisoquinolyliene (Entry 5, Table 3),²⁴ tetrahydropyrimidinylidene (Entries 6-9, Table 3),²⁵ diazepanyliene (Entries 10-11, Table 3),^{12b, 26} diaminomethylidene (Entries 12-14, Table 3),²⁷ cyclic (alkyl)(amino)carbene (CAAC) (Entries 15-17, Table 3),²⁸ cyclic (amino)(aryl)carbene (CAArC) (Entry 18, Table 3),²⁹ 1,2,4-triazolylidene (Entries 19-23, Table 3),^{14b, 30} abnormal NHC (Entries 24-26, Table 3)³¹ and pyrazolylidene ligands (Entry 27, Table 3).³²

From Table 3 it can be appreciated that increased buried

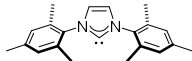
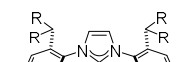

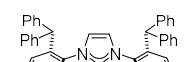
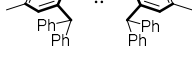
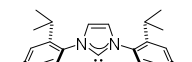

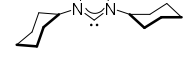
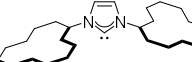
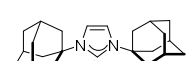
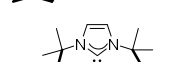
Entry	[AuCl(NHC)]	Abbreviation	Reference/ CCDC	% V_{bur} for M-NHC length at	
				2.00 Å	2.28 Å
1		IMes	14b 263603	36.5	31.2
2		IPent (R = Et)	11b 926491	49.0	43.4
3		IHept (R = Pr)	11d 977384	51.2	47.0
4		INon (R = Bu)	11d 977385	51.3	47.1
5		IPr*	19 836612	50.4	45.7
6		IPr ^{OMe} (R = OMe)	11c 987701	45.6	40.0
7		IPr ^{NH2} (R = NH ₂)	20 1061936	46.5	40.9
8		ICy	14b 250396	27.5	23.6
9		IDD	21b 679915	32.2	27.9
10		IAd	14b 263609	39.8	35.3
11		I ^t Bu	21a 247531	39.6	35.1

Table 2. Systematic modifications on the *N*-substituents of selected NHC ligands and their steric impact on the corresponding [AuCl(NHC)] species.

volumes can be achieved when a rigid core can force a substituent downwards at a suitable angle; for example, Entries 1, 3, and 4 have very large % V_{bur} due to this effect. In addition, CAAC and CAArC ligands tend to have very large percent buried volumes because of the quaternary sp^3 centre that replaces what would be an *NR* substituent in an imidazol-2-ylidene scaffold. However, the motivation for using these ligands is not necessarily due to their steric properties; species such as those in Entries 6-8 (with a pyrimidalised nitrogen) and Entries 15-17 (CAAC ligands) have interesting and useful electronic properties, such as reduced π -accepting ability.³³

Many of the ligands shown in Table 3 are unsymmetrical, and therefore, the percent buried volume does not fully describe the steric environment that these enforce around the metal centre; this limitation can be overcome by quoting buried volumes for each quadrant around the metal, or by the use of steric maps (*vide infra*).

3. Steric Maps

3.1 Definition and Calculation

% V_{bur} provides a means of quantifying the steric profile of a given ligand, but provides limited detail regarding the special arrangement of this steric impact. To overcome this issue,

Entry	[AuCl(NHC)]	Abbreviation	Reference/ CCDC	%V _{bur} for M-NHC length at		Entry	[AuCl(NHC)]	Abbreviation	Reference/ CCDC	%V _{bur} for M-NHC length at	
				2.00 Å	2.28 Å					2.00 Å	2.28 Å
1			23a 921409	49.2	45.6	15			28a 671265	47.9	42.8
2			23b 1430678	26.0	22.4	16			28b 723865	51.0	45.7
3		(R = Ad)	23c 1060572	53.0	49.2	17			28c 1494597	53.8	49.4
4		(R = Dipp)	23d 1444424	54.1	49.9	18			29 1056559	36.5	32.4
5			24 782788	33.2	28.7	19			14b 263610	27.7	24.1
6		(R = Dipp)	25a 924514	38.5	33.9	20			30a 743804	32.9	29.0
7		(R = Mes)	25b 1427003	34.4	29.6	21			30b 1011248	33.5	29.2
8		(R = CH ₂ SO ₂ Tol)	25b 1427004	36.2	31.6	22			30c 1443075	31.3	27.4
9			25c 1444061	55.9	52.0	23			30d 641267	33.9	29.6
10		THD-Mes	12b 892182	42.9	37.6	24		(R = Ad)	31 855898	34.3	30.6
11			26 782382	47.1	42.0	25		(R = PMP)	31 855900	28.4	25.0
12			27 766153	36.9	32.6	26			31 855899	29.4	25.4
13			27 766154	34.7	30.6	27			32 637547	23.5	20.3
14			27 766163	37.5	33.2						

Table 3. Summary of %V_{bur} for a series of gold(I) complexes bearing uncommon or exotic NHC ligands.

different sets of descriptors, such as the sterimol parameters, have been proposed.³⁴ Although these approaches have been proven to be extremely useful for correlating a given structural feature to catalytic activity, they do not showcase a clear picture of the catalytic pocket. Therefore, Cavallo and coworkers conceived a new and complementary concept, the steric maps,^{8c} to overcome this limitation and provide a way to represent and visualise the steric profile of – particularly unsymmetrical – NHC ligands, *inter alia*.

Steric maps show, *via* coloured contours, the steric bulk that is presented to the metal centre, and divides it into quadrants. These are visualised looking along the bond between the metal

centre and the carbene carbon (see Figure 5). These allow an appreciation of how the steric impact of the ligand is distributed throughout space; i.e. this might be evenly spread, or one or more areas may contain most of the steric bulk. This allows the identification of features such as catalytic pockets, or might allow for the origin of enantioselectivity to be identified for some catalysts. For example, as shown in Figure 5 for [AuCl(ITrop)],³⁵ both South East (SE) and North West (NW) quadrants are heavily hindered by the ligand (%V_{bur} = 62.2 and 44.7, respectively); thus, in catalysis, this ligand would allow substrates to approach preferentially from the South West (SW) or North East (NE) positions (%V_{bur} = 28.3 or 38.4, respectively).

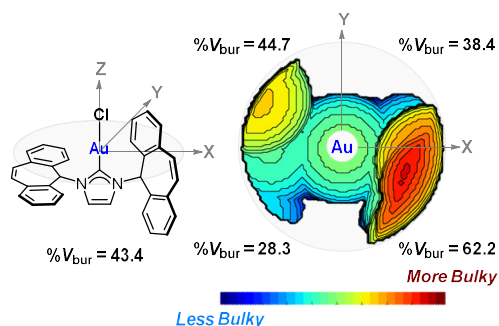


Figure 5. % V_{bur} vs Steric map representation of [AuCl(IITrop)]

3.2 Scope and Limitations

SambVca 2.0^{8d} can be used to simultaneously calculate the % V_{bur} and steric maps of a given species. The required input is the same in order to calculate both parameters: a CIF or XYZ file with the atomic co-ordinates of either the ligand of interest or the complete complex. While the % V_{bur} condenses the overall steric impact of a given ligand into a single descriptor, the steric maps offer a *per quadrant* representation of the steric hindrance around the metal centre, thus providing a better picture of the catalytic pocket. This could be particularly useful for complexes bearing unsymmetrical or chiral ligands.

To illustrate how steric maps can help to better rationalise the steric impact of a given ligand, both steric maps and % V_{bur} for selected gold(I)-NHC species were calculated and compared (Table 4). Entries 1 and 2 in Table 4,³⁶ show two unsymmetrical complexes, bearing *N*-Mes and *N*-alkyl substituents, which have the same overall % V_{bur} of 34.5 (for an Au-NHC length of 2.00 Å); thus, making it difficult to understand the difference between the steric profiles of these ligands from this descriptor alone. The subtle differences between these two ligands can better be understood by looking at their corresponding steric maps. From these it is clear that, for example, for the ligand bearing a *N*-cyclodecyl substituent (Entry 1) the northern quadrants (NE, NW) are more hindered; therefore, a substrate might approach from the SE or SW. However, in the case of the second NHC (Entry 2) both SE and NW quadrants are more sterically congested, thus forming a diagonal axis from where the substrate can approach the metal centre. Another example of how steric maps can help us to better understand the steric environment around a metal centre can be seen for unsymmetrical complexes bearing bulky yet highly flexible *N*-substituent, such as Trop (Entries 3–5, Table 4).³⁵ There, it can be appreciated how the *N*-Trop substituent can easily adapt itself to the steric requirements of the complex, thanks to the free rotation around the CN bond. This can lead to complexes where the Trop group is perpendicular (Entries 3 and 5, Table 4) or parallel to the XY plane (Entry 4, Table 4). Depending on the orientation of the Trop group, both % V_{bur} and steric maps can present dramatic variations. This can be seen, for example, when comparing the % V_{bur} between the complexes bearing a *N*-adamantyl and *N*-methyl substituents in Entries 4 and 5. The theoretically bulkier ligand, with a *N*-adamantyl group, has a lower % V_{bur} than the one bearing a *N*-methyl group (37.7 vs

Entry	[AuCl(NHC)]	Steric map representation ^a	% V_{bur} for M-NHC length at	
			2.00 Å	2.28 Å
1			40.9	36.8
			33.6	26.8
2			27.0	39.0
			45.7	26.1
3			37.6	43.3
			49.2	74.4
4			39.9	30.6
			43.1	36.7
5			25.9	65.5
			26.5	43.0

Table 4. Selected examples of [AuCl(NHC)] species and their corresponding % V_{bur} and Steric maps. ^a Calculated for Au-NHC length of 2.00 Å.

40.2); the same trend can be observed when looking at their steric maps. These examples also help to highlight the main limitation of these descriptors, which is that they only consider ligand conformations in the solid state. This is perfectly valid when studying a very rigid system where conformational changes will have a limited impact on the steric environment in solution, but it could lead to misinterpretations when dealing with highly flexible substituents. Therefore, even though both descriptors are very useful to help researchers to better understand the environment around a metal centre, they should be analysed with caution when dealing with flexible ligands.

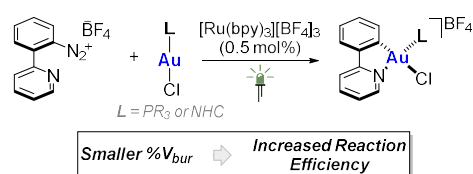
4. Application of % V_{bur} and Steric Maps in Catalysis Mediated by Transition Metals

The main function of molecular descriptors is to help researchers understand and rationalise reactivity trends. In this regard, both % V_{bur} and steric maps have been used, as stand-alone parameters or in combination with other descriptors, to further understand chemical processes. In this section we would like to disclose some selected examples covering a variety of areas, ranging from stoichiometric organometallic chemistry to catalytic transformations, where the use of either % V_{bur} or steric maps helped to elucidate reactivity trends. Recent work at the forefront of catalysis by researchers such as

Milo and Sigman has used a range of parameters to understand selectivity and reactivity in catalysis,³⁷ but % V_{bur} and steric maps are more straightforward and accessible ways to identify trends in catalysis.

4.1 Oxidative Addition to Gold

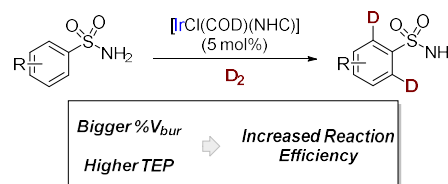
Recently, Glorius and coworkers have expanded their work on the combination of gold(I) and photoredox catalysis with a mechanistic study on the oxidative addition of aryl-diazonium salts, bearing a pendant pyridine moiety, to Au^I species; these reactions afford (C,N)-cyclometalated Au^{III} complexes (Scheme 1).³⁸ With this work they intended to validate their mechanistic hypothesis, where a Au^I species was oxidized by a photogenerated aryl radical to Au^{II} and then subsequently to Au^{III} in an electron transfer chain, and devise a straightforward protocol to access cationic (C,N)-cyclometalated Au^{III} complexes.^{38b} Interestingly, they observed that the reaction worked for both NHC and phosphine ligands, more or less independently of their electronic properties. However, the reaction proved to be quite sensitive to variations on the steric environment of the Au^I species. % V_{bur} analyses revealed that the efficiency of the reaction decreased with an increase in buried volume. The authors conclude that this observation likely explains the poor catalytic activity of gold(I) complexes with % V_{bur} > 44 in their original report.³⁹



Scheme 1. Oxidative addition to Au^I by photoredox catalysis.

4.2 Iridium-catalysed Hydrogen Isotope Exchange

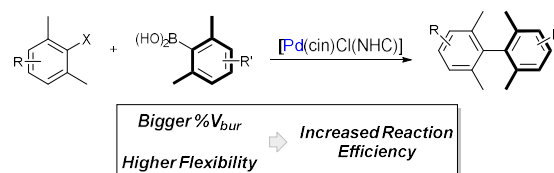
Another example of the use of % V_{bur} to understand catalytic activity was reported by Kerr and Tuttle in 2014.⁴⁰ They reported the use of [IrCl(COD)(NHC)] species to perform CH activation and deuteration of primary sulphonamides (Scheme 2). There, they used a combination of % V_{bur} and the Tolman electronic parameter (TEP) to help them understand the reactivity trends and ultimately select the best catalyst. Their study revealed that non-bulky catalysts, where the ligand had % V_{bur} < 33%, were inactive in this transformation. The authors hypothesised that this observation was consistent with their belief that bulky substituents help to achieve an efficient reductive elimination step, thus favouring the overall process. In addition, the use of the TEP helped them to elucidate the difference in reactivity between NHC ligands with similar steric environments, and suggested that more electron rich ligands boosted reactivity. All the above considerations lead them to select [IrCl(COD)(IMes^{Me})] as the catalyst of choice for the CH activation and deuteration of sulfonamides.⁴⁰



Scheme 2. CH activation and deuteration of sulfonamides by [IrCl(COD)(NHC)] species.

4.3 Palladium-catalysed Cross-Coupling

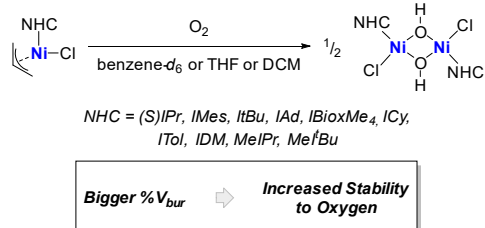
For the last decade, many groups have been interested on the synthesis of Pd-NHC complexes and the study of their reactivity in cross-coupling reactions.⁴¹ It has been observed that the use of bulky, electron rich ligands helped promote challenging transformations, such as the synthesis of tetra-substituted biaryl species.^{41b, 42} In 2012 the synthesis and reactivity studies of [Pd(η^3 -cinnamyl)Cl(IPr*)] was reported (Scheme 3).⁴³ Studies revealed that this ligand was the most active for this transformation under mild reaction conditions, when compared to other prominent bulky NHC ligands such as IPent or (*anti*-(2,7)-SiCyoctNap). A careful evaluation and comparison of the % V_{bur} and Steric maps of [Pd(η^3 -cinnamyl)Cl(NHC)] (NHC = IPr, SiPr, IPr* and *anti*-(2,7)-SiCyoctNap) revealed that, although IPr* was the bulkiest NHC reported for catalytically active [Pd(η^3 -cinnamyl)Cl(NHC)] species, it is also quite flexible and can adapt its shape to the surrounding environment. A careful examination of the steric maps also revealed that [Pd(η^3 -cinnamyl)Cl(IPr*)] possesses two highly hindered quadrants, with the other two being less sterically congested. It was hypothesised that the latter are the route of approach for the substrates, allowing the formation of the key intermediate [Pd(Ar)(Ar')(IPr*)], while the two bulkier quadrants might influence and facilitate the reductive elimination step and thus the product formation.⁴³



Scheme 3. Use of [Pd(η^3 -cinnamyl)Cl(NHC)] for cross-coupling reactions.

4.4 Oxidation of Nickel Pre-catalysts

Sigman reported a profound steric effect on the reactivity of [Ni(η^3 -allyl)Cl(NHC)] complexes with oxygen.⁴⁴ Solutions of the nickel species with many NHC ligands were found to lead to the formation of [NiCl(μ -OH)(NHC)]₂ dimers (Scheme 4). It was found that *t*Bu and IAd complexes were highly stable to oxygen, with no reaction observed after 48 h in benzene, THF, or DCM. In contrast, complexes bearing NHCs such as IPr, SiPr, and IMes underwent reaction within seconds (in benzene or THF), with the ICy complex being slightly more stable (*ca.* 5 min in benzene). % V_{bur} for [Ni(CO)₃(NHC)] complexes were used to establish the trend in steric bulk *versus* reactivity, but values



Scheme 4. Oxidation of [Ni(allyl)Cl(NHC)] complexes by molecular oxygen.

can also be calculated for the [Ni(η^3 -allyl)Cl(NHC)] complexes that are known (at 2.00/2.28Å: *t*Bu: 37.8/33.5; IBioxMe₄: 31.2/27.0; IPr: 37.0/31.8);⁴⁴⁻⁴⁵ these values agree qualitatively with the observation that the *t*Bu complex is stable to oxygen and the other two complexes are not.

4.5 Dynamic Behaviour of Intermediates in Ruthenium-Catalysed Alkene Metathesis

Cavallo and co-workers used dynamics calculations to assess the flexibility of NHCs.⁴⁶ The distribution of different conformers was assessed, and the percent buried volume of each conformer was calculated; Figure 6 illustrates the effect of the *N*-substituent on the steric impact of the ligand in the [RuCl₂(NHC)(CH₂)] complex. This overcomes one of the key limitations of the use of X-ray data to assess buried volumes. Notably, both the average %V_{bur} and the range of %V_{bur} vary considerably between ligands. The IPh derivative (**V**) and the IMes derivative (**I**) have approximately the same average %V_{bur} but the IPh derivative covers a much larger range.

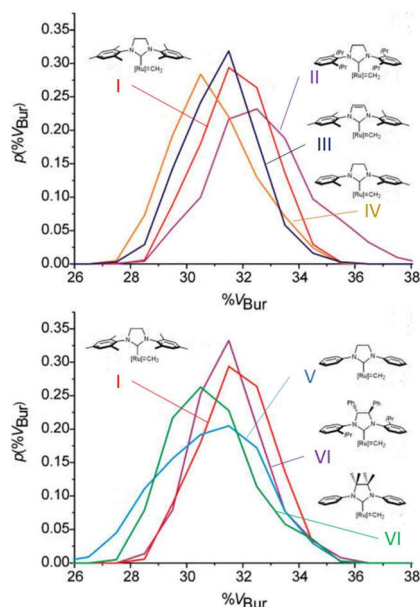


Figure 6. Dynamic behaviour of [RuCl₂(NHC)(CH₂)] complexes; reproduced with permission from reference 46.

4.6 Understanding Enantioselective Catalysis

An underexplored application of steric maps is in catalysis using chiral NHCs or complexes thereof. Chiral NHCs have found a

number of applications,⁴⁷ most notably in hydrogenation.⁴⁸ Unfortunately, the use of catalyst systems formed *in situ* means there is a lack of good structural data for these types of complexes. However, a few examples from the literature can be considered. IBioxMe₄ and IBiox[(-)-menthyl] have the same rigid backbone but different pendant groups. Chaplin has reported the structure of [RhCl(CO)₂(IBioxMe₄)]⁴⁹ while Lautens has reported [RhCl(CO)₂(IBiox[(-)-menthyl])]; the latter complex is an effective catalyst for the enantioselective hydroarylation of alkenes using boronic acid substrates.⁵⁰ The catalytic pockets in each of these complexes can be visualised using steric maps, showing that the achiral complex is very open, with little difference in the steric impact of each quadrant, while the rhodium centre in the chiral complex clearly has only limited accessibility (Figure 7; the measured Rh-C distances were used).

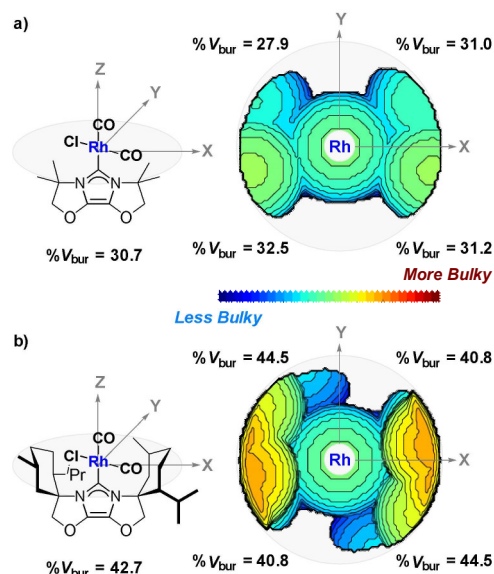
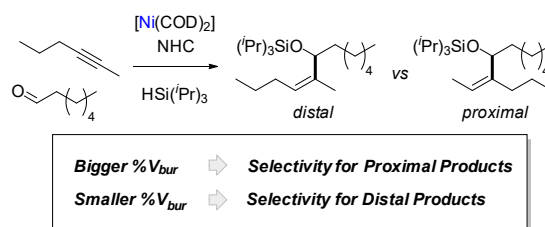


Figure 7. Visualising the spatial arrangement of steric impact in (a) [RhCl(CO)₂(IBioxMe₄)] and (b) [RhCl(CO)₂(IBiox[(-)-menthyl])].

4.7 Regioselectivity Switching in Nickel-Catalysed Reductive Couplings of Aldehydes and Alkynes

Houk and Montgomery have used DFT methods to understand why the regioselectivity of reductive alkyne/aldehyde coupling reactions switches with different NHCs;⁵¹ larger and smaller NHCs produce different products (Scheme 5).



Scheme 5. Oxidation of [Ni(allyl)Cl(NHC)] complexes by molecular oxygen.

While DFT calculations could reproduce the observed regioselectivity relatively well, there was not a simple relationship between %V_{bur} and regioselectivity. A complete

understanding of ligand effects required the use of 2D contour maps of the van der Waals surface (Figure 8). The *isopropyl* substituents on IPr were found to protrude into an area of space where they clashed with substituents on the alkyne, while IAd and ITol presented most of their steric bulk in a different region.

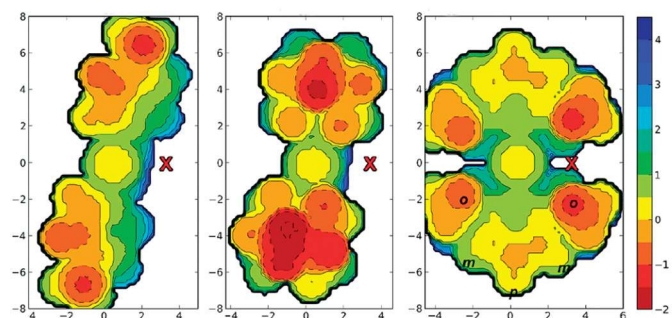


Figure 8. Visualising the steric impact of NHCs attached to nickel catalysts; from left to right: ITol, IAd, IPr. The red X represents where the distal substituent of the alkyne sits. Image reproduced from reference 51 with permission.

5. Conclusions and Outlook

Two key methods to analyse and quantify the steric impact of *N*-heterocyclic carbene (NHC) ligands have been presented and discussed. The *percent buried volume* ($\%V_{bur}$) provides a convenient single number to measure the overall steric impact of a ligand; *steric maps* provide a graphical representation of the steric profile of a ligand using colour-coded contour maps and also provide *per quadrant* information of the steric impact of the ligand. The former is the most used to date and it is a good descriptor to compare the overall steric impact of NHC ligands; the latter provides a better picture of the ligands' steric contour and its impact on the catalytic pocket. Both methodologies are useful descriptors to guide our understanding and comparison of the steric demand of NHC ligand. However, their main limitation is intrinsic to the way they are calculated: both parameters require the use of a CIF or XYZ file with the atomic co-ordinates of either the ligand of interest or the complete complex. This means that they describe the steric impact of the most thermodynamically stable conformation of the ligand, or that which is favoured under the crystallisation conditions, and so they are not completely representative of behaviour in solution. While one must be careful when interpreting results from $\%V_{bur}$ calculations and steric maps, especially when dealing with flexible ligands, these remain two of the most conceptually simple, easy-to-use, and powerful ways of exploring the steric properties of NHCs.

Acknowledgements

DJN thanks the University of Strathclyde for a Chancellor's Fellowship.

Biographies



Adrián Gómez-Suárez received his Licenciatura (Masters) in Chemistry from the University of Santiago de Compostela in 2009 and then undertook a research stay at the University of Heidelberg in the group of Prof. A. Stephen K. Hashmi. In 2014 he was awarded his PhD from the University of St. Andrews for his studies on the stoichiometric and catalytic chemistry of dinuclear gold complexes under the supervision of Prof. Steven P. Nolan FRSE. Since early 2015 he has been a Postdoctoral fellow in the group of Prof. Frank Glorius at Westfälische Wilhelms-Universität Münster. His research interests include organometallic chemistry, catalysis and photochemistry.



David Nelson graduated from the University of Edinburgh in 2008 with an MChem in Chemistry with Industrial Experience which included research at AstraZeneca and with the late Professor Hamish McNab. He was awarded his PhD from the University of Strathclyde in 2012 for research on structure/activity relationships in alkene metathesis with Professor Jonathan M. Percy. He spent two years at the University of St Andrews, working with Professor Steven P. Nolan FRSE on a range of topics in organometallic chemistry and catalysis. Since mid-2014 he has been a Lecturer and Chancellor's Fellow at the University of Strathclyde, where he is exploring structure/activity relationships and mechanisms in cross-coupling and C-H activation reactions.



Steven P. Nolan received his BSc in Chemistry from the University of West Florida and his PhD from the University of Miami where he worked under the supervision of Professor Carl D. Hoff. After a postdoctoral stay with Professor Tobin J. Marks at Northwestern University, he joined the Department of Chemistry of the University of New Orleans in 1990. In 2006, he joined the Institute of Chemical Research of Catalonia (ICIQ). In early 2009, he joined the School of Chemistry at the University of St Andrews. In 2015 he moved to the University of Ghent. His research interests include organometallic chemistry and homogeneous catalysis.

Abbreviations

%V _{bur}	percent buried volume
Ad	adamantyl
bpy	2,2'-bipyridine
CAAC	cyclic (alkyl)amino carbene
CAArC	cyclic amino(aryl) carbene
CIF	crystallographic information file
cin	cinnamyl
COD	1,5-cyclooctadiene
Dipp	2,6-di- <i>iso</i> -propylphenyl
IAd	1,3-diadamantyylimidazol-2-ylidene
IBioxMe ₄	3,3,7,7-tetramethyl-2,3,7,8-tetrahydroimidazol[4,3- <i>b</i> :5,1- <i>b'</i>]bis(oxazole)-4-ylidene
ICy	1,3-dicyclohexylimidazol-2-ylidene
IDD	1,3-dicyclododecylimidazol-2-ylidene
IDM	1,3-dimethylimidazol-2-ylidene
IDM ^{Cl}	1,3-bismethyl-4,5-dichloroimidazol-2-ylidene
IDM ^{Me}	1,3-bismethyl-4,5-dimethylimidazol-2-ylidene
IHept	1,3-bis(2,6-di(4-heptyl)phenyl)imidazol-2-ylidene
I <i>i</i> Pr	1,3-bis(<i>iso</i> propyl)imidazol-2-ylidene
I <i>i</i> Pr ^{Benz}	1,3-bis(<i>iso</i> propyl-benzimidazol-2-ylidene
IMes	1,3-dimesitylimidazol-2-ylidene
IMes ^{Me}	1,3-dimesityl-4,5-dimethylimidazol-2-ylidene
INon	1,3-bis(2,6-di(5-nonyl)phenyl)imidazol-2-ylidene
IPent	1,3-bis(2,6-di(3-pentyl)phenyl)imidazol-2-ylidene
IPh	1,3-diphenylimidazol-2-ylidene
IPr	1,3-bis(2,6-di- <i>iso</i> -propylphenyl)imidazol-2-ylidene
IPr ^{Cl}	1,3-bis(2,6-di- <i>iso</i> -propylphenyl)-4,5-dichloroimidazol-2-ylidene
IPr ^{Me}	1,3-bis(2,6-di- <i>iso</i> -propylphenyl)-4,5-dimethylimidazol-2-ylidene
IPr ^{NH₂}	1,3-bis(2,6-di- <i>iso</i> propyl-4-aminophenyl)imidazol-2-ylidene
IPr ^{OMe}	1,3-bis(2,6-di- <i>iso</i> propyl-4-methoxyphenyl)imidazol-2-ylidene
IPr [*]	1,3-bis(2,6-bis(diphenylmethyl)-4-methylphenyl)imidazol-2-ylidene
I ^t Bu	1,3-di(<i>tert</i> -butyl)imidazol-2-ylidene
ITent	"tentacular" imidazol-2-ylidenes
ITol	1,3-bis(4-methylphenyl)imidazol-2-ylidene
ITrop	1,3-bis(5H-dibenzo[<i>a,d</i>]cyclohepten-5-yl)imidazol-2-ylidene
MeIPr	1-methyl-3-(2,6-di- <i>iso</i> propyl)imidazol-2-ylidene
MeI ^t Bu	1-methyl-3-(<i>tert</i> -butyl)imidazol-2-ylidene
Mes	mesityl; 1,3,5-trimethylphenyl
NHC	<i>N</i> -heterocyclic carbene
PMP	<i>para</i> -methoxyphenol
SICyoctNap	<i>N,N'</i> -bis(2,7-bis(dicyclooctyl)naphthalen-1-yl)imidazol-2-ylidene
SI <i>i</i> Pr	1,3-bis(<i>iso</i> propyl-4,5-dihydroimidazol-2-ylidene
SIMes	1,3-dimesityl-4,5-dihydroimidazol-2-ylidene

SIPr	1,3-bis(2,6-di- <i>iso</i> -propylphenyl)-4,5-dihydroimidazol-2-ylidene
TEP	Tolman electronic parameter
THD-Dipp	1,3-bis(2,6-di- <i>iso</i> propylphenyl)-3,4,5,6-tetrahydrodiazepin-2-ylidene
THD-Mes	1,3-bis(2,4,6-methylphenyl)-3,4,5,6-tetrahydrodiazepin-2-ylidene
THP-Dipp	1,3-bis(aryl)-3,4,5,6-tetrahydropyrimidin-2-ylidene
Trop	5H-dibenzo[<i>a,d</i>]cyclohepten-5-yl

Notes and references

- M. N. Hopkinson, C. Richter, M. Schedler and F. Glorius, *Nature*, 2014, **510**, 485-496.
- S. Díez-González, N. Marion and S. P. Nolan, *Chem. Rev.*, 2009, **109**, 3612-3676.
- D. M. Flanagan, F. Romanov-Michailidis, N. A. White and T. Rovis, *Chem. Rev.*, 2015, **115**, 9307-9387.
- T. Dröge and F. Glorius, *Angew. Chem. Int. Ed.*, 2010, **49**, 6940-6952.
- D. J. Nelson and S. P. Nolan, *Chem. Soc. Rev.*, 2013, **42**, 6723-6753.
- H. Clavier and S. P. Nolan, *Chem. Commun.*, 2010, **46**, 841-861.
- C. A. Tolman, *Chem. Rev.*, 1977, **77**, 313-348.
- (a) A. C. Hillier, W. J. Sommer, B. S. Yong, J. L. Petersen, L. Cavallo and S. P. Nolan, *Organometallics*, 2003, **22**, 4322-4326; (b) A. Poater, B. Cosenza, A. Correa, S. Giudice, F. Ragone, V. Scarano and L. Cavallo, *Eur. J. Inorg. Chem.*, 2009, 1759-1766; (c) A. Poater, F. Ragone, R. Mariz, R. Dorta and L. Cavallo, *Chem. Eur. J.*, 2010, **16**, 14348-14353; (d) L. Falivene, R. Credendino, A. Poater, A. Petta, L. Serra, R. Oliva, V. Scarano and L. Cavallo, *Organometallics*, 2016, **35**, 2286-2293.
- N. Fey, M. F. Haddow, J. N. Harvey, C. L. McMullin and A. G. Orpen, *Dalton Trans.*, 2009, 8183-8196.
- (a) D. S. Surry and S. L. Buchwald, *Angew. Chem. Int. Ed.*, 2008, **47**, 6338-6361; (b) R. Martin and S. L. Buchwald, *Acc. Chem. Res.*, 2008, **41**, 1461-1473.
- (a) J. Balogh, A. M. Z. Slawin and S. P. Nolan, *Organometallics*, 2012, **31**, 3259-3263; (b) A. Collado, J. Balogh, S. Meiries, A. M. Z. Slawin, L. Falivene, L. Cavallo and S. P. Nolan, *Organometallics*, 2013, **32**, 3249-3252; (c) D. J. Nelson, A. Collado, S. Manzini, S. Meiries, A. M. Z. Slawin, D. B. Cordes and S. P. Nolan, *Organometallics*, 2014, **33**, 2048-2058; (d) S. R. Patrick, A. Collado, S. Meiries, A. M. Z. Slawin and S. P. Nolan, *J. Organomet. Chem.*, 2015, **775**, 152-154.
- (a) P. Hauwert, J. J. Dunsford, D. S. Tromp, J. J. Weigand, M. Lutz, K. J. Cavell and C. J. Elsevier, *Organometallics*, 2013, **32**, 131-140; (b) O. S. Morozov, A. V. Lunchev, A. A. Bush, A. A. Tukov, A. F. Asachenko, V. N. Khrustalev, S. S. Zaleskiy, V. P. Ananikov and M. S. Nechaev, *Chem. Eur. J.*, 2014, **20**, 6162-6170; (c) R. C. Poulten, I. López, A. Llobet, M. F. Mahon and M. K. Whittlesey, *Inorg. Chem.*, 2014, **53**, 7160-7169; (d) A. R. Leverett, A. I. McKay and M. L. Cole, *Dalton Trans.*, 2015, **44**, 498-500; (e) J. J. Dunsford, D. J. Evans, T. Pugh, S. N. Shah, N. F. Chilton and M. J. Ingleson, *Organometallics*, 2016, **35**, 1098-1106; (f) S. Pelties, E. Carter, A. Folli, M. F. Mahon, D. M.

- Murphy, M. K. Whittlesey and R. Wolf, *Inorg. Chem.*, 2016, **55**, 11006-11017.
13. (a) M. R. Fructos, T. R. Belderrain, P. de Frémont, N. M. Scott, S. P. Nolan, M. M. Díaz-Requejo and P. J. Pérez, *Angew. Chem. Int. Ed.*, 2005, **44**, 5284-5288; (b) S. Gaillard, X. Bantreil, A. M. Z. Slawin and S. P. Nolan, *Dalton Trans.*, 2009, 6967-6971; (c) S. Gaillard, A. M. Z. Slawin, A. T. Bonura, E. D. Stevens and S. P. Nolan, *Organometallics*, 2010, **29**, 394-402.
14. (a) H. M. J. Wang, C. S. Vasam, T. Y. R. Tsai, S.-H. Chen, A. H. H. Chang and I. J. B. Lin, *Organometallics*, 2005, **24**, 486-493; (b) P. de Frémont, N. M. Scott, E. D. Stevens and S. P. Nolan, *Organometallics*, 2005, **24**, 2411-2418; (c) E. Schuh, C. Pflüger, A. Citta, A. Folda, M. P. Rigobello, A. Bindoli, A. Casini and F. Mohr, *J. Med. Chem.*, 2012, **55**, 5518-5528; (d) V. W.-W. Yam, J. K.-W. Lee, C.-C. Ko and N. Zhu, *J. Am. Chem. Soc.*, 2009, **131**, 912-913; (e) L. Kaps, B. Biersack, H. Müller-Bunz, K. Mahal, J. Münzner, M. Tacke, T. Mueller and R. Schobert, *J. Inorg. Biochem.*, 2012, **106**, 52-58.
15. (a) M. B. E. Griffiths, S. E. Koponen, D. J. Mandia, J. F. McLeod, J. P. Coyle, J. J. Sims, J. B. Giorgi, E. R. Sirianni, G. P. A. Yap and S. T. Barry, *Chem. Mater.*, 2015, **27**, 6116-6124; (b) M. V. Baker, P. J. Barnard, S. J. Berners-Price, S. K. Brayshaw, J. L. Hickey, B. W. Skelton and A. H. White, *J. Organomet. Chem.*, 2005, **690**, 5625-5635; (c) R. Jothibas, H. V. Huynh and L. L. Koh, *J. Organomet. Chem.*, 2008, **693**, 374-380.
16. (a) S. Flügge, A. Anoop, R. Goddard, W. Thiel and A. Fürstner, *Chem. Eur. J.*, 2009, **15**, 8558-8565; (b) J. J. Dunsford, K. J. Cavell and B. M. Kariuki, *Organometallics*, 2012, **31**, 4118-4121.
17. M. Tobisu, A. Yasutome, H. Kinuta, K. Nakamura and N. Chatani, *Org. Lett.*, 2014, **16**, 5572-5575.
18. J. Yau, K. E. Hunt, L. McDougall, A. R. Kennedy and D. J. Nelson, *Beilstein J. Org. Chem.*, 2015, **11**, 2171-2178.
19. A. Gómez-Suárez, R. S. Ramón, O. Songis, A. M. Z. Slawin, C. S. J. Cazin and S. P. Nolan, *Organometallics*, 2011, **30**, 5463-5470.
20. W. J. Ramsay, J. A. Foster, K. L. Moore, T. K. Ronson, R. J. Mirgalet, D. A. Jefferson and J. R. Nitschke, *Chem. Sci.*, 2015, **6**, 7326-7331.
21. (a) M. V. Baker, P. J. Barnard, S. K. Brayshaw, J. L. Hickey, B. W. Skelton and A. H. White, *Dalton Trans.*, 2005, 37-43; (b) N. Marion, G. Lemièrre, A. Correa, C. Costabile, R. S. Ramón, X. Moreau, P. de Frémont, R. Dahmane, A. Hours, D. Lesage, J.-C. Tabet, J.-P. Goddard, V. Gandon, L. Cavallo, L. Fensterbank, M. Malacria and S. P. Nolan, *Chem. Eur. J.*, 2009, **15**, 3243-3260.
22. G. C. Fortman, A. M. Z. Slawin and S. P. Nolan, *Dalton Trans.*, 2010, **39**, 3923-3930.
23. (a) M. Kriechbaum, G. Winterleitner, A. Gerisch, M. List and U. Monkowius, *Eur. J. Inorg. Chem.*, 2013, **2013**, 5567-5575; (b) M. Mihorianu, M. H. Franz, P. G. Jones, M. Freytag, G. Kelter, H.-H. Fiebig, M. Tamm and I. Neda, *Appl. Organomet. Chem.*, 2016, **30**, 581-589; (c) M. Espina, I. Rivilla, A. Conde, M. M. Díaz-Requejo, P. J. Pérez, E. Álvarez, R. Fernández and J. M. Lassaletta, *Organometallics*, 2015, **34**, 1328-1338; (d) Y. Kim, Y. Kim, M. Y. Hur and E. Lee, *J. Organomet. Chem.*, 2016, **820**, 1-7.
24. D. Hirsch-Weil, K. A. Abboud and S. Hong, *Chem. Commun.*, 2010, **46**, 7525-7527.
25. (a) M. J. Lopez-Gomez, D. Martin and G. Bertrand, *Chem. Commun.*, 2013, **49**, 4483-4485; (b) X. Hu, D. Martin, M. Melaimi and G. Bertrand, *J. Am. Chem. Soc.*, 2014, **136**, 13594-13597; (c) T. Wurm, F. Mulks, C. R. N. Böhring, D. Riedel, P. Zargaran, M. Rudolph, F. Rominger and A. S. K. Hashmi, *Organometallics*, 2016, **35**, 1070-1078.
26. T. W. Hudnall, A. G. Tennyson and C. W. Bielawski, *Organometallics*, 2010, **29**, 4569-4578.
27. A. S. K. Hashmi, T. Hengst, C. Lothschütz and F. Rominger, *Adv. Synt. Catal.*, 2010, **352**, 1315-1337.
28. (a) G. D. Frey, R. D. Dewhurst, S. Kousar, B. Donnadiu and G. Bertrand, *J. Organomet. Chem.*, 2008, **693**, 1674-1682; (b) X. Zeng, G. D. Frey, R. Kinjo, B. Donnadiu and G. Bertrand, *J. Am. Chem. Soc.*, 2009, **131**, 8690-8696; (c) J. Chu, D. Munz, R. Jazzar, M. Melaimi and G. Bertrand, *J. Am. Chem. Soc.*, 2016, **138**, 7884-7887.
29. B. Rao, H. Tang, X. Zeng, L. Liu, M. Melaimi and G. Bertrand, *Angew. Chem. Int. Ed.*, 2015, **54**, 14915-14919.
30. (a) M. Alcarazo, T. Stork, A. Anoop, W. Thiel and A. Fürstner, *Angew. Chem. Int. Ed.*, 2010, **49**, 2542-2546; (b) J. Turek, I. Panov, P. Svec, Z. Ruzickova and A. Ruzicka, *Dalton Trans.*, 2014, **43**, 15465-15474; (c) C. Thie, S. Hitzel, L. Wallbaum, C. Bruhn and U. Siemeling, *J. Organomet. Chem.*, 2016, **821**, 112-121; (d) C. Dash, M. M. Shaikh, R. J. Butcher and P. Ghosh, *Inorg. Chem.*, 2010, **49**, 4972-4983.
31. A. S. K. Hashmi, D. Riedel, M. Rudolph, F. Rominger and T. Oeser, *Chem. Eur. J.*, 2012, **18**, 3827-3830.
32. F. Kessler, N. Szesni, C. Maaß, C. Hohberger, B. Weibert and H. Fischer, *J. Organomet. Chem.*, 2007, **692**, 3005-3018.
33. (a) O. Back, M. Henry-Ellinger, C. D. Martin, D. Martin and G. Bertrand, *Angew. Chem. Int. Ed.*, 2013, **52**, 2939-2943; (b) A. Liske, K. Verlinden, H. Buhl, K. Schaper and C. Ganter, *Organometallics*, 2013, **32**, 5269-5272; (c) S. V. C. Vummaleti, D. J. Nelson, A. Poater, A. Gómez-Suárez, D. B. Cordes, A. M. Z. Slawin, S. P. Nolan and L. Cavallo, *Chem. Sci.*, 2015, **6**, 1895-1904; (d) K. Verlinden, H. Buhl, W. Frank and C. Ganter, *Eur. J. Inorg. Chem.*, 2015, **2015**, 2416-2425.
34. (a) K. B. Lipkowitz, C. A. D'Hue, T. Sakamoto and J. N. Stack, *J. Am. Chem. Soc.*, 2002, **124**, 14255-14267; (b) K. Angermund, W. Baumann, E. Dinjus, R. Fornika, H. Görls, M. Kessler, C. Krüger, W. Leitner and F. Lutz, *Chem. Eur. J.*, 1997, **3**, 755-764; (c) K. C. Harper and M. S. Sigman, *J. Org. Chem.*, 2013, **78**, 2813-2818; (d) K. C. Harper, S. C. Vilardi and M. S. Sigman, *J. Am. Chem. Soc.*, 2013, **135**, 2482-2485.
35. M. Brill, A. Collado, D. B. Cordes, A. M. Z. Slawin, M. Vogt, H. Grützmaier and S. P. Nolan, *Organometallics*, 2015, **34**, 263-274.
36. P. Queval, C. Jahier, M. Rouen, I. Artur, J.-C. Legeay, L. Falivene, L. Toupet, C. Crévisy, L. Cavallo, O. Baslé and M. Mauduit, *Angew. Chem. Int. Ed.*, 2013, **52**, 14103-14107.
37. M. S. Sigman, K. C. Harper, E. N. Bess and A. Milo, *Acc. Chem. Res.*, 2016, **49**, 1292-1301.
38. (a) M. N. Hopkinson, A. Tlahuext-Aca and F. Glorius, *Acc. Chem. Res.*, 2016, **49**, 2261-2272; (b) A. Tlahuext-Aca, M. N.

- Hopkinson, C. G. Daniliuc and F. Glorius, *Chem. Eur. J.*, 2016, **22**, 11587-11592.
39. B. Sahoo, M. N. Hopkinson and F. Glorius, *J. Am. Chem. Soc.*, 2013, **135**, 5505-5508.
40. W. J. Kerr, M. Reid and T. Tuttle, *ACS Catal.*, 2015, **5**, 402-410.
41. (a) G. C. Fortman and S. P. Nolan, *Chem. Soc. Rev.*, 2011, **40**, 5151-5169; (b) C. Valente, S. Çalimsiz, K. H. Hoi, D. Mallik, M. Sayah and M. G. Organ, *Angew. Chem. Int. Ed.*, 2012, **51**, 3314-3332.
42. F. Izquierdo, S. Manzini and S. P. Nolan, *Chem. Commun.*, 2014, **50**, 14926-14937.
43. A. Chartoire, M. Lesieur, L. Falivene, A. M. Z. Slawin, L. Cavallo, C. S. J. Cazin and S. P. Nolan, *Chem. Eur. J.*, 2012, **18**, 4517-4521.
44. B. R. Dible and M. S. Sigman, *Inorg. Chem.*, 2006, **45**, 8430-8441.
45. B. R. Dible and M. S. Sigman, *J. Am. Chem. Soc.*, 2003, **125**, 872-873.
46. F. Ragone, A. Poater and L. Cavallo, *J. Am. Chem. Soc.*, 2010, **132**, 4249-4258.
47. F. Wang, L.-j. Liu, W. Wang, S. Li and M. Shi, *Coord. Chem. Rev.*, 2012, **256**, 804-853.
48. D. Zhao, L. Candish, D. Paul and F. Glorius, *ACS Catal.*, 2016, **6**, 5978-5988.
49. A. B. Chaplin, *Organometallics*, 2014, **33**, 3069-3077.
50. J. Bexrud and M. Lautens, *Org. Lett.*, 2010, **12**, 3160-3163.
51. P. Liu, J. Montgomery and K. N. Houk, *J. Am. Chem. Soc.*, 2011, **133**, 6956-6959.

Graphical TOC

